Stress Corrosion Cracking Susceptibility of Precipitation-Hardening Nickel Base Alloys Under Simulated Hot, Deep, Sour Gas Well Downhole Environments

Ho Jin Choi
IITRI Westport Technology Center International
6700 Portwest Drive
Houston, Texas 77024

ABSTRACT

Threshold temperatures below which stress corrosion cracking (SCC) does not occur were determined for various precipitation-hardening (PH) alloys, 718, 725, 625+ (age-hardenable) and HIP 625 (powder metallurgy). Slow strain rate tests (SSRT) were performed in a range of temperatures (350 - 400 °F) in a 25% NaCl solution pressurized with gases to simulate a deep, hot, sour gas well in Gulf of Mexico (10 psi H_2S + 500 psi CO_2). Threshold temperatures to SCC were obtained for the four alloys. An experimental procedure of SSRT is discussed in terms of deaeration procedure and other experimental artifacts. Dissolved oxygen drastically affected SCC of I-718 as did H_2S.

Key Word: stress corrosion cracking, SCC, slow strain rate test, SSRT, hydrogen sulfide, sour service

INTRODUCTION

Two alloy families have been widely used in the oil industry for completing deep sour gas wells which produce high partial pressures of hydrogen sulfide, carbon dioxide and hot brine: cold-worked (CW) and precipitation-hardening (PH) non-ferrous alloys such as nickel base alloys. Conventional carbon steels are extremely susceptible to both localized corrosion and weight loss corrosion under deep, hot, sour downhole environments. Both alloy systems can easily meet the strength requirements for completing deep wells (normally greater than 100 ksi yield strength at room temperature), however, significant differences in their physical properties and reaction to service environments dictate their specific applications.

Alloys which are cold-worked exhibit superior resistance over PH alloys to both weigh loss and localized corrosion such as pitting corrosion, crevice corrosion and

Superalloys 718, 625, 706 and Various Derivatives
Edited by E.A. Loria
The Minerals, Metals & Materials Society, 1994

stress corrosion cracking (SCC). The inferior performance of PH alloys is attributed to the fact they contain areas of localized stress buildup around precipitates which form in their metallurgical grain structure. These precipitates are the primary reason for this group of alloys' high strength properties.

While CW alloys have better corrosion resistance, they are limited in size due to manufacturing restrictions; PH alloy tubular does not have this limitation. In addition, PH alloys are easily machined while precision machining of CW alloys is difficult because of the stored energy that frequently causes dimensional distortion during machining. Thus, many drilling engineers opt to choose PH alloys for use over CW alloys in manufacturing downhole assemblies including packer assemblies and subsurface safety valves. CW alloys have been primarily used for downhole production tubulars. Recent developments in powder metallurgy technology provide another method of producing downhole materials: hot isostatic pressing (HIP) requires a rigorous process control to minimize precipitation of improper compounds. HIP 625 would be a suitable material for use as a tubing hanger in the hot sour well if it can cope with the hot and sour downhole's corrosive fluid.

The objective of this work was to determine the SCC susceptibility of various PH alloys (718. 725, 625+) for use in hot, deep, sour service environments. HIP 625 was additionally tested for comparison. Resistance to SCC was determined by a slow strain rate test (SSRT).

EXPERIMENTAL

Test Materials

Four PH alloys were selected for testing: I-718, I-725, 625+ and HIP 625. Table 1 lists chemical compositions and mechanical properties of test materials.

Specimen Preparation

A SSRT specimen of 1.27-cm gauge length and 0.381-cm gauge diameter was machined from stock materials supplied from alloy producers. A wet-600 grit SiC paper was used to polish the surface of a SSRT specimen. A SSRT specimen was degreased with acetone, washed with distilled water and dried in air.

Test Apparatus

A 500-ml Hastelloy C-276 autoclave vessel was used. A SSRT specimen was electrically isolated from the vessel by using a Teflon gland. Both the top and bottom pull rods were also electrically isolated from the SSRT machine by using a Zirconium oxide coated holder that was wrapped with Teflon tape. Three SSRT machines were employed in this work. Each SSRT machine was calibrated to have a strain rate of 4×10^{-6}/sec. The compliance of the test machine was within the acceptable limit of the slope of the load/time plot in accordance with the proposed NACE standard.

Test Conditions

One of the Gulf-of-Mexico's reservoir conditions was simulated: 25% NaCl brine, 500 psi CO_2 and 10 psi H_2S. Temperature varied from 425 °F to 300 °F until no SCC occurred. At first I-718 was tested and test temperatures for the rest of the test materials were selected based on the results of I-718 testing.

Data Analysis

Visual/scanning electron microscopic (SEM) examination and ductility measurements were conducted. Three ductility parameters were measured and compared to corresponding data determined in air: Time-to-failure (TTF), Elongation and Reduction area. TTF is the time to fracture from zero load. The zero load was derived from extrapolation of the elastic portion of the load-time curves to zero load. Among them, TTF appeared to be most consistent and thus TTF was selected to determine the threshold temperature. Finally, each fracture surface was examined by SEM.

RESULTS & DISCUSSION

In the 25% NaCl solution, most of the test alloys (I-725, 625+ and HIP 625) exhibited only marginal evidence of SCC or were immune to SCC under the test condition. But I-718 demonstrated varying degree of the susceptibility to SCC, and its susceptibility depended upon temperature. Increasing temperature accelerated the susceptibility to SCC of I-718, whereas I-725, 625+ showed only marginal cracking on the fracture surface without any secondary cracks on the side surface of SSRT specimens. HIP 625 started to show the susceptibility to SCC at 400 °F but below 400 °F it was immune to SCC.

Figure 1 is the TTF ratio vs. temperature for I-718, I-725, 625+ and HIP 625 tested in 25% NaCl under 10 psi H_2S + 500 psi CO_2 at temperatures from 300 to 425 °F. The elongation of I-718 was drastically reduced in the test solution with increasing temperature, indicating a threshold temperature of less than 300 °F. In contrast, I-715, 625+ exhibited good ductility and resistance to SCC up to 375 and 350 °F, respectively. Of the four alloys, I-725 performed the best under the test conditions. HIP 625 appeared to perform slightly less than 625+ at 400 °F but was not subject to SCC at temperatures lower than 375 °F. Thus, a threshold temperature for HIP 625 was 375 °F, greater than that of 625+.

Figure 2 shows a typical scanning electron microscopic (SEM) fractograph of a HIP 625 SSRT specimen strained at 400 °F exhibiting SCC on the fracture surface. After examining the fracture surfaces under both stereo scope and SEM, the threshold temperatures (means no SCC on the primary fracture surface) were determined for the alloys in the test conditions as follows:

° I-718	less than 300 °F
° 625+	350 °F
° HIP 625	375 °F
° I-725	375 °F

One of the major features in simulating downhole conditions in a laboratory is to remove dissolved oxygen from a test fluid. Figure 3 shows load vs. time curves for I-718 SSRT specimens tested at three different concentrations of dissolved oxygen in a test fluid. As shown in Figure 3, I-718 was subject to severe stress corrosion cracking (SCC) in the aerated 25% NaCl solution. When the test solution was deaerated by sparging CO_2 for one hour, the SSRT specimen tested in a deaerated 25% NaCl under 500 psi CO_2 at 400 °F did not exhibit any evidence of SCC. I-718 however was highly susceptible to the aerated solution, indicating that oxygen contamination in the test solution can mislead the interpretation of the SCC resistance of this alloy. One-hour sparging with a CO_2 gas appeared to be sufficient for deaeration. Adding 10 psi H_2S into the solution drastically increased the susceptibility of I-718 to SCC. All of the SSRT specimens of I-718 did not exhibit pitting corrosion. These observations indicate that both dissolved oxygen and H_2S appear to shift the corrosion potential of the alloys into the trans-passive region, which accelerated SCC. Another aspect of residual dissolved oxygen in the test solution is to promote formation of elemental sulfur on the surface of a specimen as follows:

$$H_2S + {}^1/_2\,O_2 \dashrightarrow S^\circ + H_2O \qquad (1)$$

It is not clear what the threshold fugacity of H_2S is to form elemental sulfur or the amount sufficient to adsorb on the surface which in turn accelerates SCC. The presence of elemental sulfur does however severely restrict the application of various corrosion resistant alloys (CRA) and reduces the applicable temperature limitation of CRAs. Elemental sulfur exhibits a drastic increase in solubility in an aqueous system when H_2S is present. This action accelerates corrosion and SCC tendencies of structural materials (1-5). One proposed mechanism is that sulfur in H_2S containing brines forms either H_2S_x, HS_x, or H^+, that have the potential to lower the solution pH thereby increasing the corrosivity of brines (6-7). Iketa et al (8-9) hypothesized the geometrical effect of elemental sulfur in promoting a crevice at the interface between molten sulfur and metal thus reducing the incubation period for crack initiation and/or crack propagation. Myasaka et al (10) proposed the presence of elemental sulfur affected the cathodic reaction, that is, sulfur reduction reaction.

Field failures associated with elemental sulfur have yet to be reported, but laboratory test results indicate a drastic increase in corrosivity and cracking susceptibility to CRAs in its presence. The presence of elemental sulfur as a reactant in Equation (1), therefore, raises a critical issue regarding the validity of the aggressiveness of laboratory test results if the deaeration procedure is not proper. Without a clear understanding of the mechanism of elemental sulfur, interpretation of laboratory experiments will be conservative and quite restrictive in selection and use of CRAs.

Some of the specimens with TTF ratios greater than 0.9 exhibited a tiny crack on the fracture surface. However, their susceptibility to SCC is only marginal. Some specimens had secondary cracks close to the primary fracture surface. Using secondary cracking as an acceptance criteria may mislead one in a proper materials selection. This is because the fracture surface, oftentimes, has more than two initiation sites. One of the cracks should be considered as a secondary crack although both cracks are present on the primary crack. So, it is recommended to negate secondary cracking in an acceptance criteria. Some companies adopt secondary cracking as a rejection guideline but this practice is not proper. TTF ratio is the most consistent indicator among the current indicators (elongation, mechanical) of SCC susceptibility when specimen fabrication is consistent. Other indicators such as elongation ratio or mechanical ratios generate greater scattering than TTF ratio.

CONCLUSIONS

SSRT is an accelerated and effective test method to determine a threshold temperature of various corrosion resistant alloys for sour applications. Among the four alloys, I-725 performed the best and threshold temperatures of the alloys under the test condition were determined as follows: less than 300 °F for I-718, 350 °F for 625+, 375 °F for HIP 625 and I-725. To avoid any experimental artifacts, a proper deaeration procedure should be adopted.

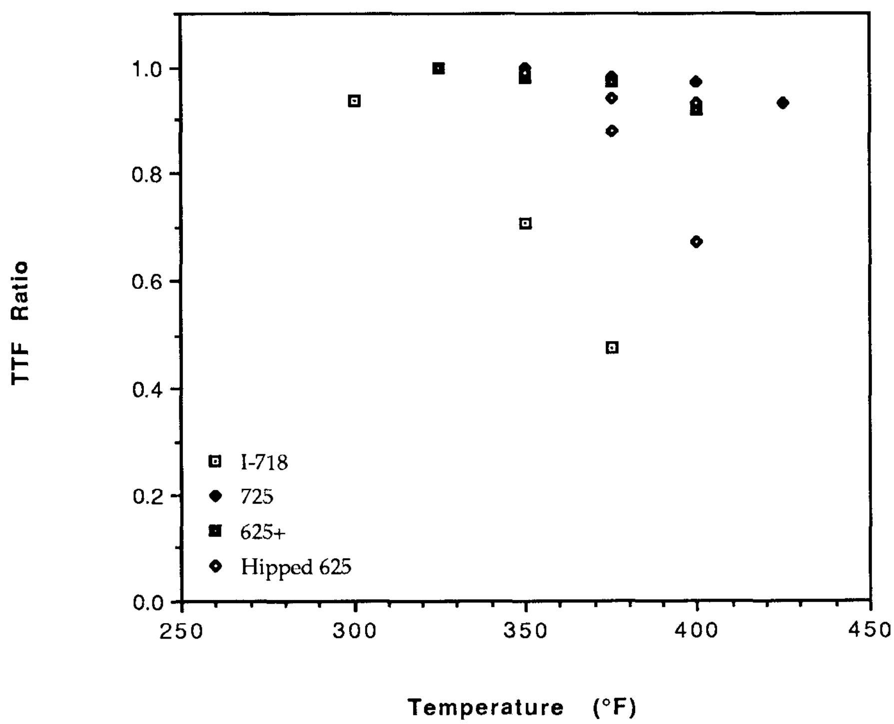

Figure 1. TTF ratio vs. temperature of I-718, I-725, 625+ and HIP 625 tested in 25% NaCl under 10 psi H_2S + 500 psi CO_2 at temperatures from 300 to 425 °F.

REFERENCES

1. Kennedy, H. T. and Wieland, D. R.: "Equilibrium in the methane-carbon dioxide-hydrogen sulfide-sulfur system," JPT (July 1960), pp. 166-69, Trans., AIME, 219

2. Roof, J. G.: "Solubility of sulfur in hydrogen sulfide and in carbon disulfide at elevated temperature and pressure," SPEJ (September 1971), pp. 272-76, Trans., AIME, 251

3. Swift, S .C., Manning, F. S., and Thompson, R. E.: "Sulfur-bearing capacity of hydrogen sulfide gas," SPEJ (April 1976), pp. 57-64, Trans., AIME, 261

4. Brunner, E. and Woll, W. : "Solubility of sulfur in hydrogen sulfide and sour gases," SPEJ (October 1980), pp. 377-84

5. Rhodes, P. R.: "Stress cracking risks in corrosive oil and gas wells", CORROSION/86, Paper No. 322, NACE (1986)

6. Choi, H. J. : "The effect of elemental sulfur and surface condition on stress corrosion cracking of high nickel alloys under hot sour environments," Paper No. 59, Presented in CORROSION/92

7. Wilhelm, S. M.: "Effect of elemental sulfur on stress corrosion cracking of nickel base alloys in deep sour gas well production", CORROSION/88, Paper No. 77, NACE (1988)

8. Ikeda, A., Igarashi, M., Ueda, M., Okada, Y., and Tsuge, H.: "On the evaluation methods of Ni-base corrosion resistant alloy for sour gas exploration and production", CORROSION/88, Paper No. 65, NACE (1988)

9. Ueda, M, Tusge, H. and Ikeda, A.: "Influence of elemental S on corrosion behavior of CRA in H_2O-CO_2-Cl- environment", CORROSION/89, Paper No. 8, NACE (1989)

10. Miyasaka, A., Denpo, K., and Ogawa, H.: "Environmental aspects of SCC of high alloys in sour environments", CORROSION/88, Paper No. 70, NACE (1988)

Table 1. Nominal chemical compositions and mechanical properties of test materials

Alloy	Chemical Composition (%wt)					Yield strength (ksi)	Tensile strength (ksi)	Elongation (%)
	Cr	Ni	Fe	Mo	Others			
I-718	19	53	19	3	5Nb+1Ti	130	185	22
I-725	20	57	9	8	3.4Mn+0.24Al+1.4Ti	130	186	32
625+	21	60	5	8	4.5Nb+Ta,1.5Ti+Al	129	184	32
HIP625	21.6	61.7	1.1	8.9	3.8Nb+0.26Ti+0.28Al	106	158	36

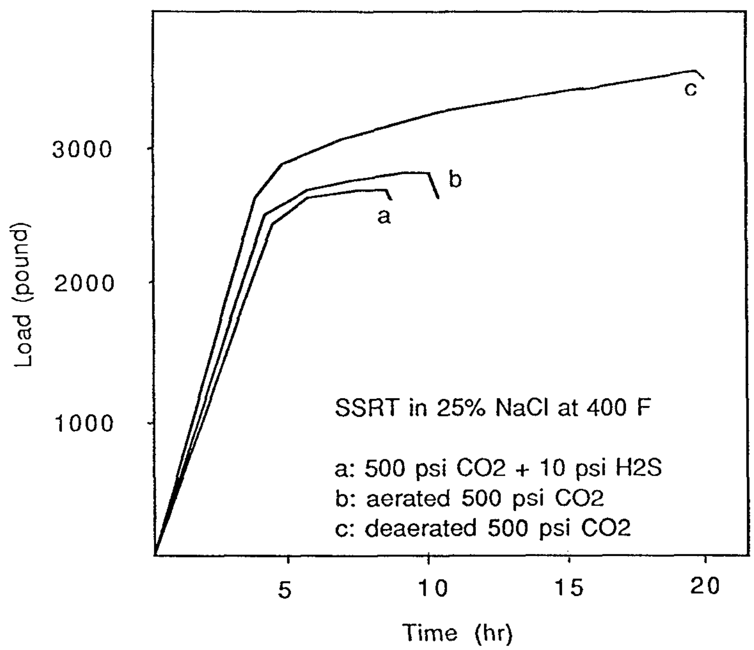

Figure 3. The effect of dissolved oxygen and H_2S (deaeration procedure) on load vs. time curves of I-718 SSRT specimens tested in 25% NaCl at 400 °F

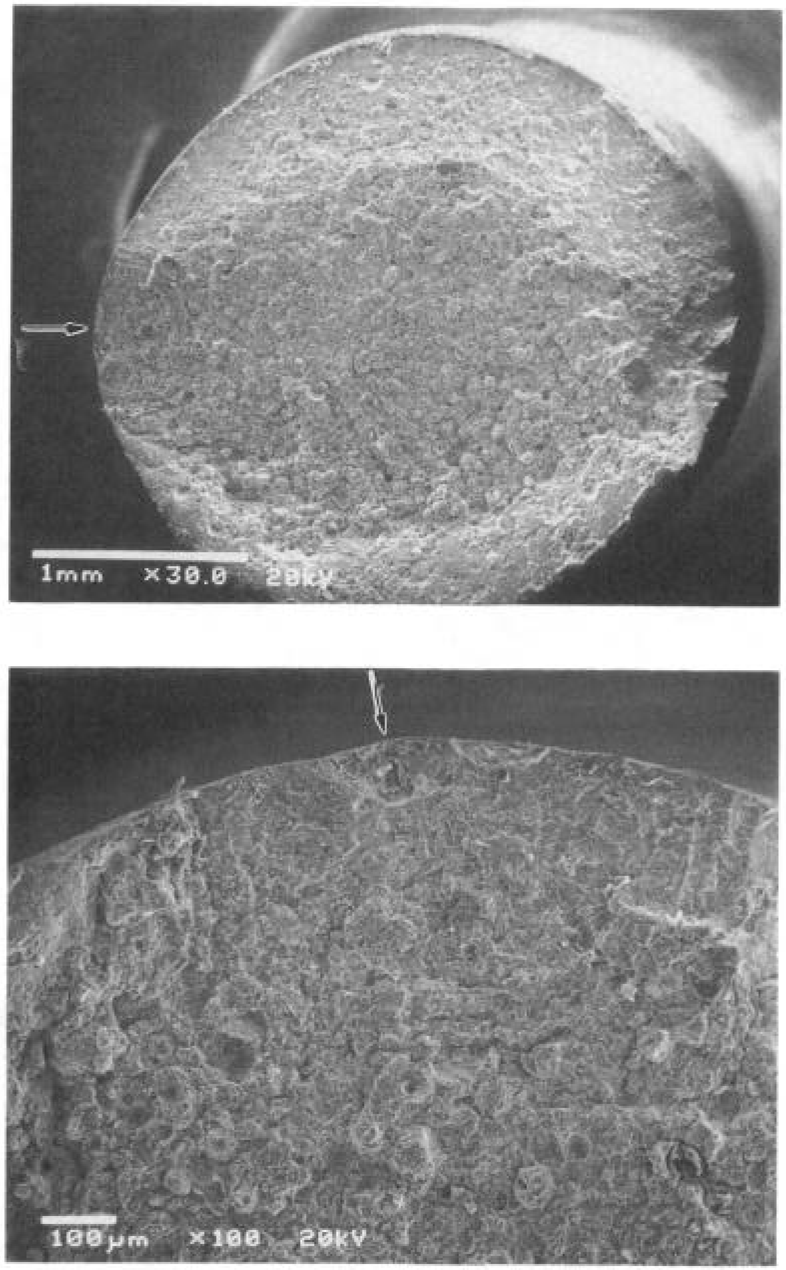

Figure 2. SEM fractographs of SSRT specimens of HIP 625 tested in 25% NaCl under 10 psi H_2S + 500 psi CO_2 at 400 °F

(a) low magnification (x30)
(b) high magnification of the SCC (x200)